MICROGRAVITY SCIENCE REVIEW

AT

NATIONAL AERONAUTICS & SPACE ADMINISTRATION
GEORGE C. MARSHALL SPACE FLIGHT CENTER
MARSHALL SPACE FLIGHT CENTER, ALABAMA 35812

February 10 - 12, 1987

GROWTH OF GaAs CRYSTALS FROM THE MELT IN A PARTIALLY CONFINED CONFIGURATION

(Contract No. NAS8-36604)

Submitted by
Professor Harry C. Gatos
and
Dr. Jacek Lagowski
Department of Materials Science and Engineering
Massachusetts Institute of Technology
Cambridge, Massachusetts 02139

Abstract

Our experimental approach has been directed along two main goals (1) the implementation of a novel approach to melt growth in a partially confined configuration; and (2) the investigation of point defect interactions and electronic characteristics as related to thermal treatment following solidification and stoichiometry. Significant progress has been made along both fronts. Crystal growth of GaAs in triangular ampuls has already been carried out successfully and consistent with our model. In fact, pronounced surface tension phenomena which cannot be observed in ordinary confinement systems have been identified and should permit the assessment of Maragoni effects prior to space processing. Regarding thermal treatment, we have discovered that the rate of cooling from elevated temperatures is primarily responsible for a whole class of defect interactions affecting the electronic characteristics of GaAs and that stoichiometry plays a critical role in the quality of GaAs.

INTRODUCTION - MOTIVATION

The advantages of near-zero gravity conditions in materials processing in general and solidification (crystal growth) in particular have been demonstrated, at least qualitatively, in a limited number of rather primitive experiments. Valid questions, however, have been raised and remain unanswered regarding the consequences of total confinement of the melt prior to solidification (i.e., stresses resulting from volume expansion during solidification, contamination of the melt surface, and others). Total confinement could also have obscured the study of the effects of surface-driven convection (Maragoni effect) which continue to be a fundamental issue regarding materials processing in space.

An additional issue became critically evident following the analysis of the results of experiments carried out in space. The effects of near-zero gravity conditions can be quantitatively assessed only if reliable approaches and techniques are available for characterization of the system in question on earth and following processing in space. Furthermore, it is imperative that ground research addresses the study and control of all experimental parameters and conditions which could possibly interfere with the identification and assessment of the zero gravity effects and/or lead to artifacts attributable to space processing.

It was with the above questions in mind that we entered into our present program. We also gave critical consideration to the choice of the material. We chose a material which would permit the optimization of the scientific benefits resulting from the elimination of convective interference. In addition, we considered it important to address the potential technological impact that these scientific benefits might have.

THE MATERIAL

We have chosen GaAs to grow in single crystal form from the melt:

The defect structure of this semiconductor presents immense challenges regarding the nature and origin of defects, their interactions, and their effects on the critical electronic properties. The understanding of the effects of stoichiometric variations, commonly present in GaAs, is severely interfered with by gravity-induced convection during solidification. In turn, convective effects on classical segregation kinetics are usually obscured by stoichiometry variations. The defect structure and segregation kinetics influenced by thermal convection are at the same time substantively affected by Fermi statistics.

GaAs, because of its high electron mobility and direct energy gap, is the most important semiconductor for a broad spectrum of applications in optoelectronic and ultra high speed energy circuits. Next to silicon, GaAs is developing to be the most widely used semiconductor. In fact, GaAs technology is now entering the early stages of exploiting the great potential of this material. Future progress will depend on achieving crystals with reproducibly controlled defect structure to meet the increasing needs of device processing.

BACKGROUND

The following major reasons precluded the consideration of a total confinement configuration (use of a cylindrical ampul confining the melt to be solidified) for the growth of semiconductor crystals: (1) The observation of a network of ridges at the surfaces of the InSb crystals grown under total confinement in the Skylab mission (Fig. 1). The presence of such ridges interferes with the study of certain aspects of the growth process. (2) Volume expansion upon solidification in the case of semiconductors leads to stresses which interfere severely with the study of the defect structure by controllable growth conditions (thermal gradients, growth rates, cooling rates, and others). (3) The study of surface tension effects cannot be addressed if the entire surface of the melt is in contact with the confining walls of the container. (4) We have discovered in our ground-based research that stoichiometric variations are caused by thermal convection and lead to impurity segregation which is totally unrelated to the accepted classical segregation kinetics. For example, in the case of Ge and Si impurities, convective currents (stoichiometric fluctuations) lead to fluctuation in the occupation of the Ga and As sites rather than in the overall concentration of these elements in the crystal (Fig. 2). Thus, control of stoichiometry is imperative in the study of GaAs crystal growth; precise stoichiometry control can be achieved by controlling the As partial vapor pressure over the melt during solidification. Such control is obviously impossible in a total confinement configuration.

THE EXPERIMENTAL APPROACH

The experimental approach has been directed along two main goals: (a) the implementation and study of a novel configuration for crystal growth under partial confinement, and (b) the investigation of native defects interactions and the key electronic characteristics (carrier concentration and carrier mobility) as related to the thermal cycle following solidification and to stoichiometry .

Partially Confined Configuration

The novel partially confined configuration conceived for the growth of GaAs crystals from the melt in space is shown schematically in Fig. 3. The melt resulting from a cylindrical charge is confined in a triangular prism. In the absence of gravity the surface energy of the melt is minimized by acquiring a cylindrical shape. The key features of this new configuration are as follows:

1. The melt is only partially confined, i.e., the contact area between the walls of the container and the melt is minimized.
2. Large free surface of the melt and the large empty space assure efficient control of the melt composition through the melt interaction with arsenic vapor.
3. Large empty space in the container is beneficial for accommodation of the volume expansion (∿11%) taking place upon solidification of GaAs.

The growth ampul is made of quartz or pyrolytic boron nitride. Upon proper surface preparation, both of these materials exhibit highly desired non-wetting characteristics. Utilization of quartz leads to Si contamination; however, this process can be effectively suppressed by oxygen added into the growth ampul.

A Horizontal Bridgman (HB) apparatus constructed for the growth of GaAs in standard boats (Figures 4 and 5) has been adapted for our ground-based experiments with the partially-confined configuration. The apparatus has three temperature zones for achieving the desired temperatures and temperature gradients. The low temperature zone which determines the partial pressure of As over the melt is controlled by a heat pipe which leads to excellent temperature control. It should be pointed out that in this HB apparatus the viewing port to facilitate seeding has been eliminated to minimize thermal symmetry and thus minimize gradient-driven convection in the melt.

Defect Interactions Related to the Rate of Cooling

We have designed and constructed experimental facilities for the fast cooling of GaAs crystals from very high temperatures (about 1200°C) and also for annealing GaAs crystals at lower temperatures (in the vicinity of 800°C). In both instances the As vapor pressure over the crystal is being controlled and maintained under near equilibrium conditions to avoid thermal etching during heat treatment or other adverse effects.

Facilities for cutting, polishing and etching of GaAs are available in our laboratory. In addition, a wide spectrum of characterization facilities has been developed for the characterization of GaAs crystals on a micro- and macro-scale. These facilities include Hall effect measurements (over a wide range of temperatures), deep level transient spectroscopy (DLTS), photo-DLTS, infrared absorption, photoluminescence, and electron beam induced current (EBIC) spectroscopy.

RESULTS

We have carried out a series of preliminary experiments using triangular prismatic containers of BN with the side of the triangular cross section being 3 mm long. They were positioned vertically on a strip heater to minimize the effect of gravity on the lateral filling of the containers. Low melting point metal alloy wires (Pb-In-Sn) were inserted into the cavity. The wires were heated from the bottom (free ends). In all instances, upon solidification, the triangular cavity was not completely filled.

In the light of the above preliminary experiments we proceeded with the construction of triangular quartz prisms in which a cylindrical charge of GaAs with a cross-section diameter of 4 mm could be inserted (Fig. 6). Growth experiments were carried out in the HB apparatus by traversing the prismatic container through the appropriate thermal gradients.

The results of the first trial experiments are very gratifying. As shown in segments of Fig. 6, even in the Horizontal Bridgman configuration the GaAs melt does not fill the entire cavity, provided the internal surfaces of the prismatic container are properly prepared. As a result, an equilibrium As pressure is maintained over the melt.

These crystals exhibit excellent electronic characteristics (as good as we have achieved in our HB apparatus using conventional boats). In addition, however, striking surface tension phenomena were revealed. These phenomena are of an oscillatory nature. The observed oscillations had three different spacings: about 1 mm, 100 μm, and 10 μm (Figures 7 and 8).

Analysis of these oscillations was carried out by chemical etching and photoluminescence. Some results are shown in Figures 9 through 12 . It is seen that the surface morphology oscillations are clearly reflected in the chemical (etching) and electronic (photoluminescence) characteristics of the material. These results are quite recent, and their analysis is still not complete. It appears, however, that they are most likely surface tension driven from variations in surface tension which may originate in variations in melt composition and/or thermal gradients. Very preliminary and qualitative modeling shows that even small changes in surface tension can lead to substantive changes in the contact angle and thus to a cross section area of the melt. In fact, in Table I we present the results of estimated changes in surface tension which can lead to oscillation of the type observed in the crystals (see also Figures 13, 14, and 15).

In the near future we plan to continue our growth experiments with emphasis on the effect of stoichiometry on the melt as controlled by the As partial pressure. Since the As ambient minimizes contamination of the melt surface, it is expected that small variations in the stoichiometry of the melt should result in substantive variations in surface tension. In addition, we intend to introduce contaminants (e.g., oxygen) in the gas phase to study the effects of such contaminants on surface tension phenomena. We are hopeful that we will be able to attain experimentally an assessment of the effects of surface tension variations.

In parallel with the growth experiments we pursued the investigation of the cooling cycle on the final properties of GaAs crystals. In accord with our previous results we found that the cooling cycle has a profound effect on the key properties of GaAs such as resistivity, carrier concentration, carrier mobility, excess carrier lifetime, deep level traps, compensation, thermal stability, macro- and microscopic uniformity, and dislocation density.

We also found that cooling-related processes may obscure the identification of solidification-related phenomena, and they could be mistaken for segregation-related growth velocity effects.

In our experimental approach we compare crystals grown under different solidification rates with those solidified at the same rates but subjected to a different cooling rate. We concluded that the cooling rate is a far more relevant parameter than the solidification rate.

We also utilized growth in magnetic fields to identify properties affected by solidification (some results are shown in Fig. 16).

A dramatic illustration of the importance of a cooling cycle is provided by ITC GaAs, a new type of GaAs with inverted thermal conversion, which is obtained by fast cooling of a GaAs crystal from 1200°C (Fig. 17). A detailed discussion of this material discovered in our laboratory in the course of this study appeared in a recent publication (Appl. Phys. Letters 49, 892 (1986).

SUMMARY

Our novel partially confined configuration for the growth of GaAs single crystals in space has been extensively tested on the ground. Even on the ground growth proceeds with a substantial fraction of free surface. We expect that in space our configuration will approach levitation conditions with perfectly controlled ambient. In the light of the results to date we will be able to study crystal growth parameters without interference, not only from gravity driven convection, but also from confining walls. Furthermore, it will be possible to investigate in semiconductor growth the effects of surface driven variations.

Table I

INHOMOGENEITIES IN GaAs GROWN
UNDER PARTIAL CONFINEMENT

	Inhomogeneities		Estimated Surface Tension Fluctuations	
	Magnitude $\delta R/R$	Spacing	Magnitude $\delta\gamma/\gamma$	Period
Macroscopic[(a)]	5%	1 mm	5%	10 min
Intermediate[(b)]	<0.3%	50-100 μm	<1%	0.5-1 min
Microscopic[(c)]	--	10-20 μm	--	4-15 s

[(a)] Seen as changes in crystal diameter, R.

[(b)] Seen in photoluminescence and differential etching.

[(c)] Seen in differential etching.

FIGURE CAPTIONS

Figure 2. Electron concentration and ionized impurity microprofiles of Si-doped melt-grown GaAs. (a) and (b) correspond to different segments of the same crystal. n is the net free electron concentration, N_A is the concentration of Si in As sites, and N_D is the concentration of Si in Ga sites. N_A+N_D is total Si concentration. Note that variations in n are not necessarily related to variations in N_A+N_D.

Figure 3. Schematic representation of the partially-confined configuration in Horizontal Bridgman mode including the corresponding temperature profiles.

Figure 4. Horizontal Bridgman growth apparatus and thermal profile (top). The quartz ampul contains the As source, 1; a breakable seal, 2; and seal breaking weight, 3; the quartz diffusion barrier, 4; a quartz boat, 5; the GaAs seed crystal, 6; and polycrystalline GaAs, 7.

Figure 6. Top segment quartz triangular prisms containing GaAs cylindrical charge; sandblasting the internal surfaces causes the upper prism to be opaque.
Middle segment Portion of the GaAs crystal after growth; the cylindrical seed and the grown crystal are clearly delineated.
Bottom segment Cross section of crystal grown in the triangular prism container. On the left-hand side it is apparent that the melt wetted the container; on the right-hand side growth took place under clean conditions.

Figure 7. Oscillations on as-grown crystal (spacing about 1 mm).

Figure 8. Schematic representation of oscillations on crystals.

Figure 10. Oscillations revealed by profilometer scanning.

Figure 11. Oscillations revealed by profilometer scanning.

Figure 12. Photoluminescence scanning revealing oscillations in crystals grown in partially confined configuration.

Figure 13. Representation of contact angle of melt with quartz container.

Figure 14. Representation of various contact angles of melt with quartz container.

Figure 15. Illustration of surface tension changes and its effects.

Figure 16. Compensation ratio (carrier mobility) in crystal grown with magnetic field turned on periodically. The as-grown crystal exhibits no effects of the magnetic field. Upon annealing at 850°C the effects of the magnetic field become quite evident. Another manifestation of the dominant role of defect structure in GaAs.

Figure 17. Low-temperature (4.2 K) optical absorption spectra of n-type melt-grown GaAs in the spectral range of photoionization and intracenter transitions of the occupied EL2 donor. (a) As-grown crystal, (b) ITC crystal, i.e., after annealing at 1200° C for 16 h and quenching. Note elimination of EL2 absorption.

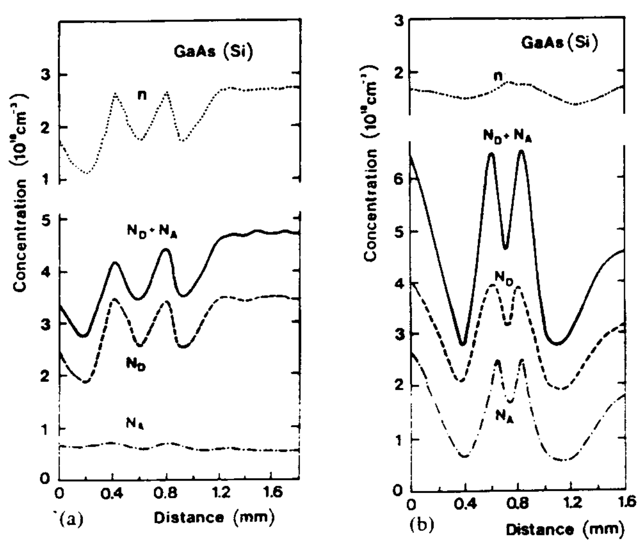
GaAs (Si)
n
N_D+N_A
N_D
N_A
Concentration (10^{16}cm^{-3})
Distance (mm)
(a)
GaAs(Si)
n
N_D+N_A
N_D
N_A
Concentration (10^{16}cm^{-3})
Distance (mm)
(b)

Figure 2.

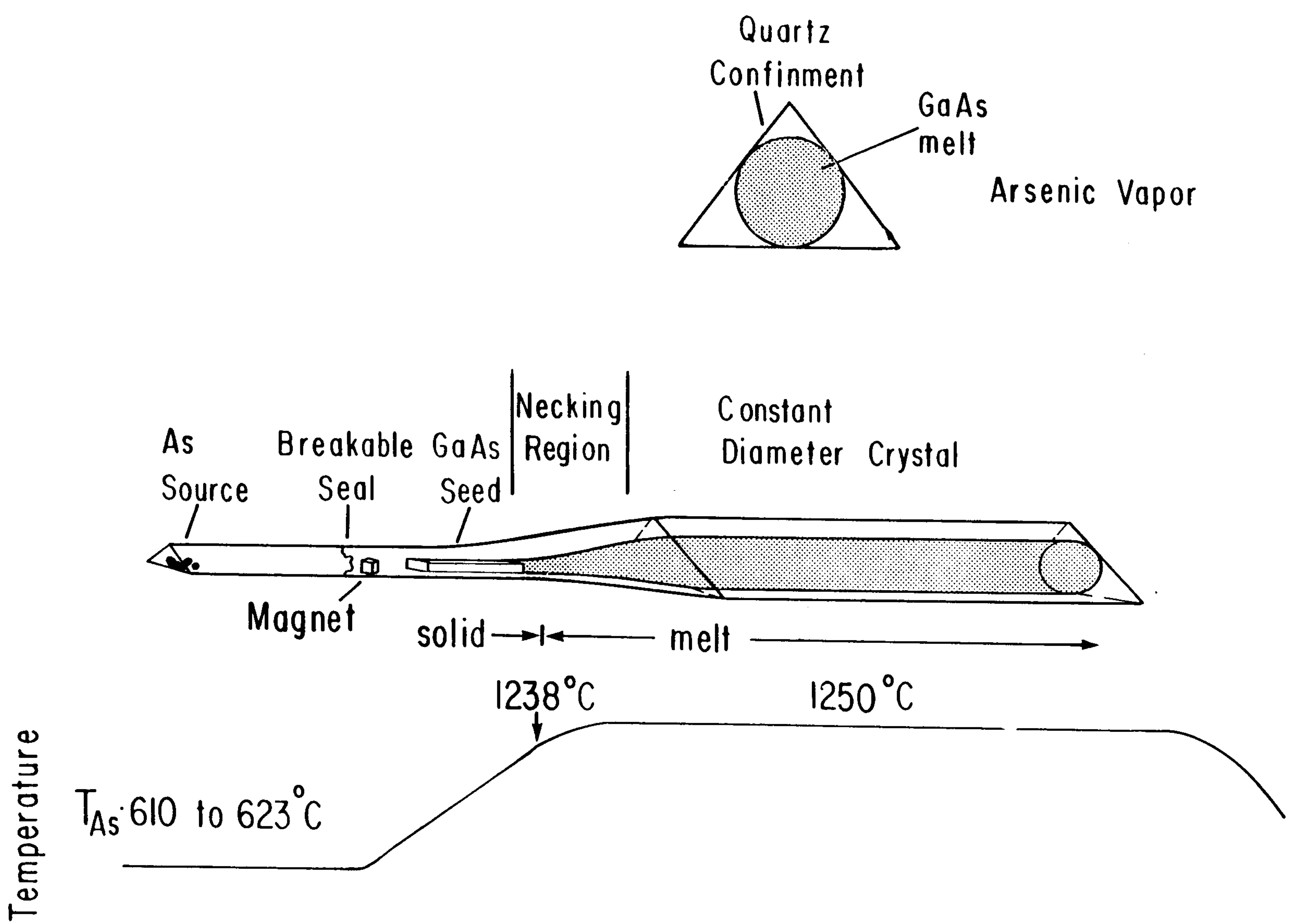

Quartz Confinment
GaAs melt
Arsenic Vapor
Necking Region
Constant Diameter Crystal
As Source
Breakable Seal
GaAs Seed
Magnet
solid
melt
1238°C
1250°C
Temperature
T_{As}: 610 to 623°C

Figure 3.

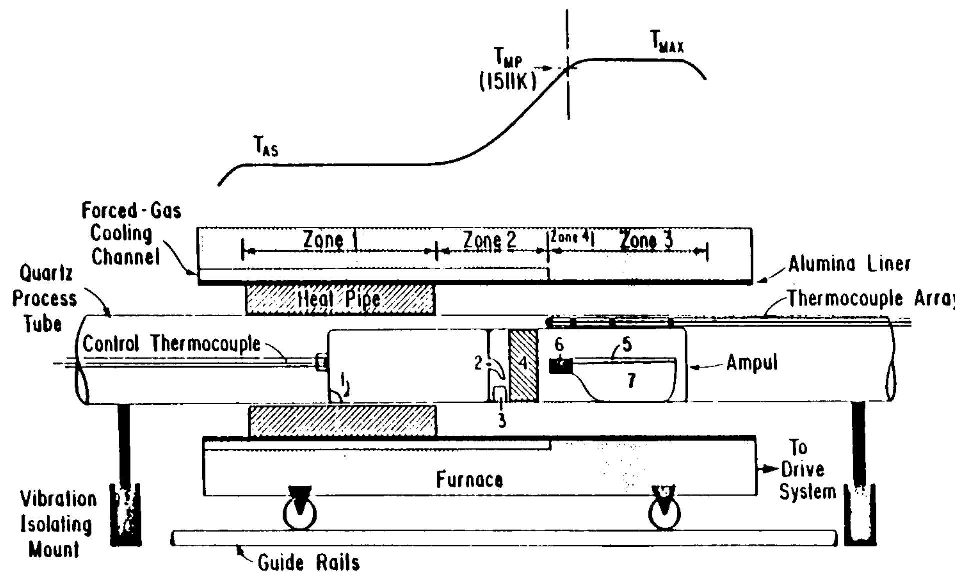
T_{MAX}
T_{MP}
(1511K)
T_{AS}
Forced-Gas
Cooling
Channel
Zone 1
Zone 2
Zone 4
Zone 3
Alumina Liner
Quartz
Process
Tube
Heat Pipe
Thermocouple Array
Control Thermocouple
1
2
3
4
5
6
7
Ampul
Furnace
To
Drive
System
Vibration
Isolating
Mount
Guide Rails

Figure 4.

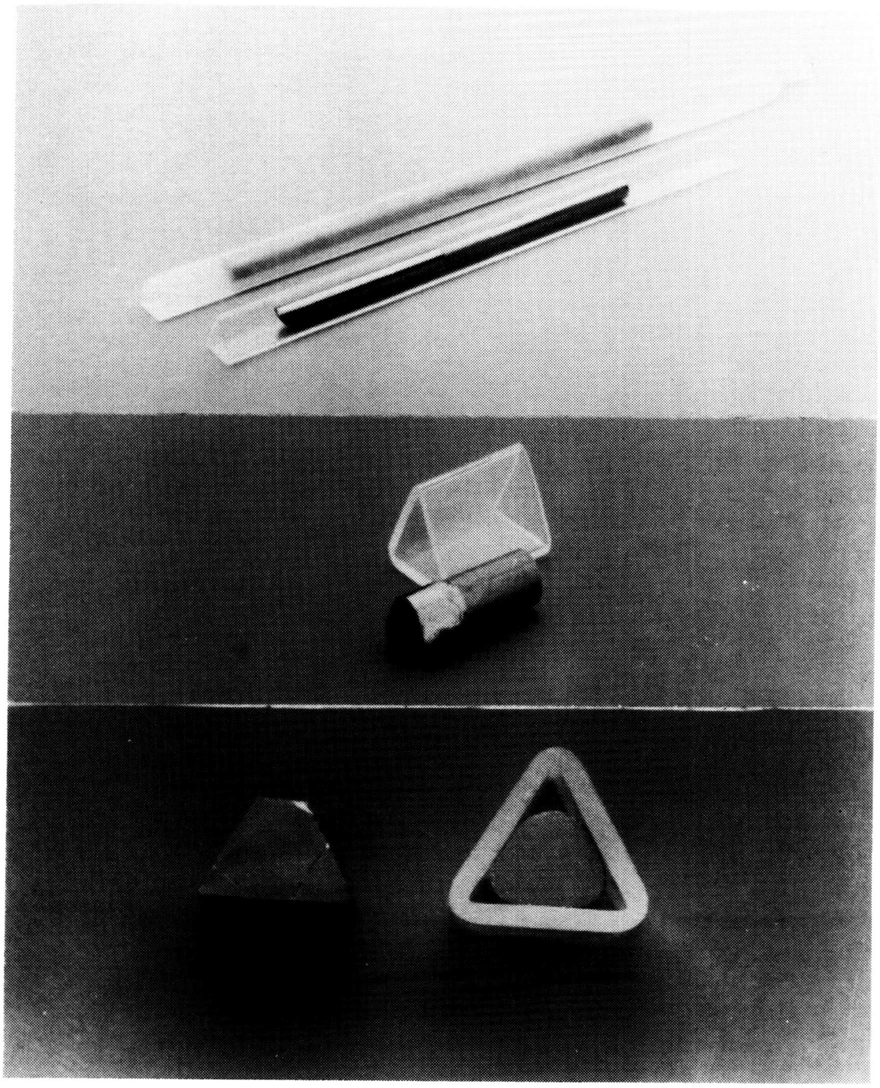

Figure 6.

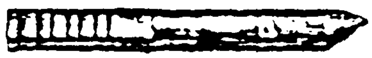

Figure 7.

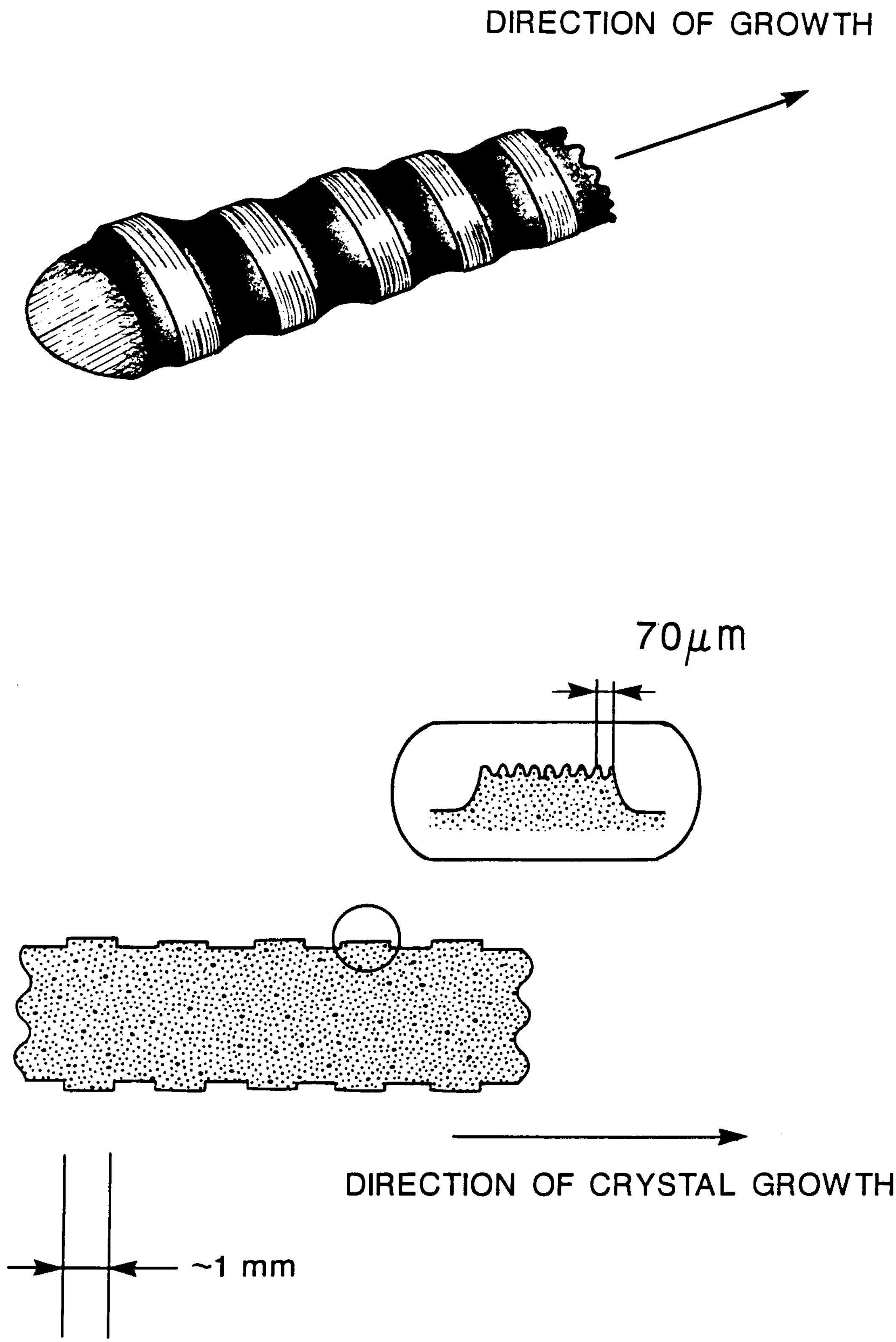

Figure 8.

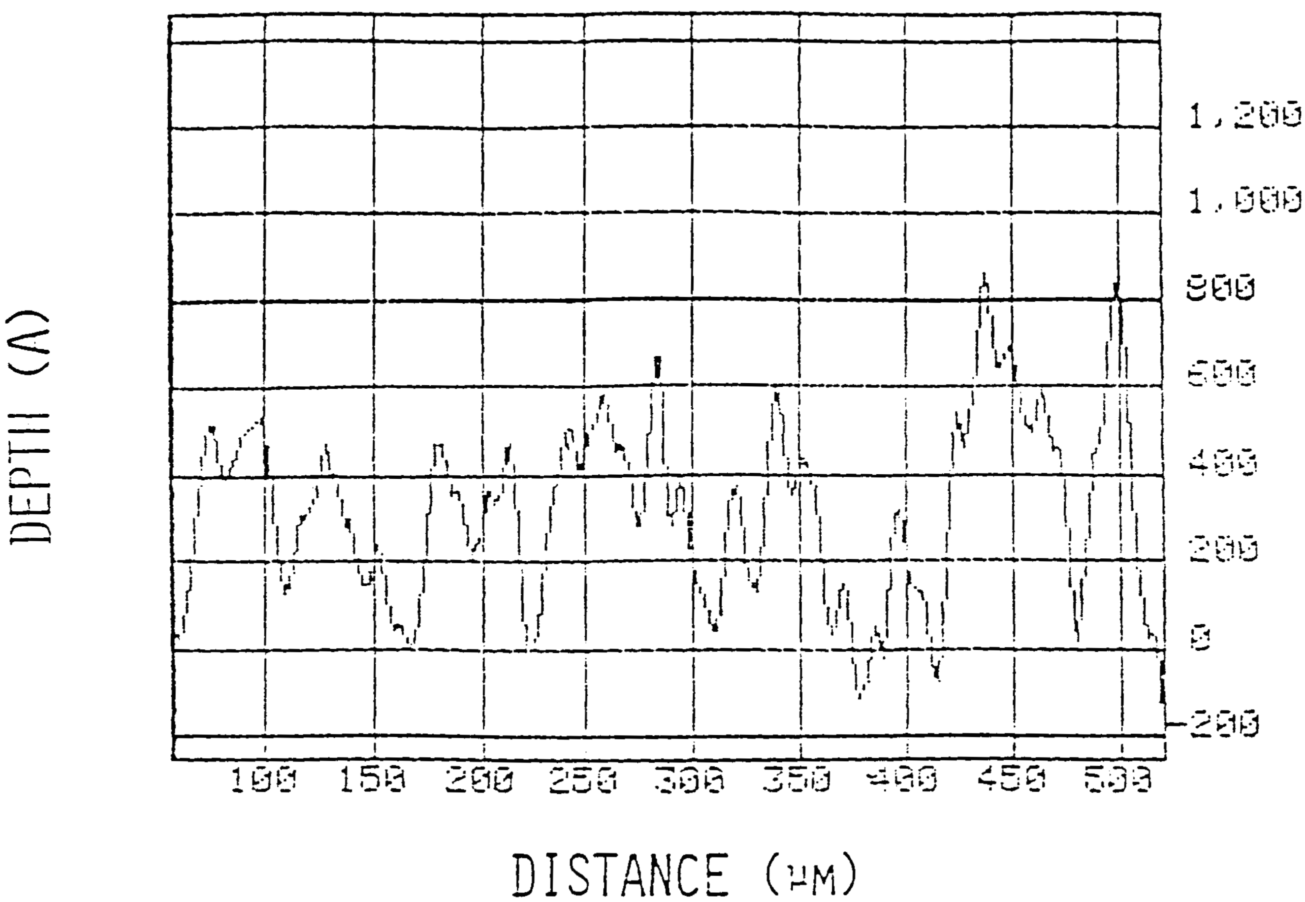
DEPTH (Å)
1,200
1,000
800
600
400
200
0
-200
100 150 200 250 300 350 400 450 500
DISTANCE (μM)

Figure 10.

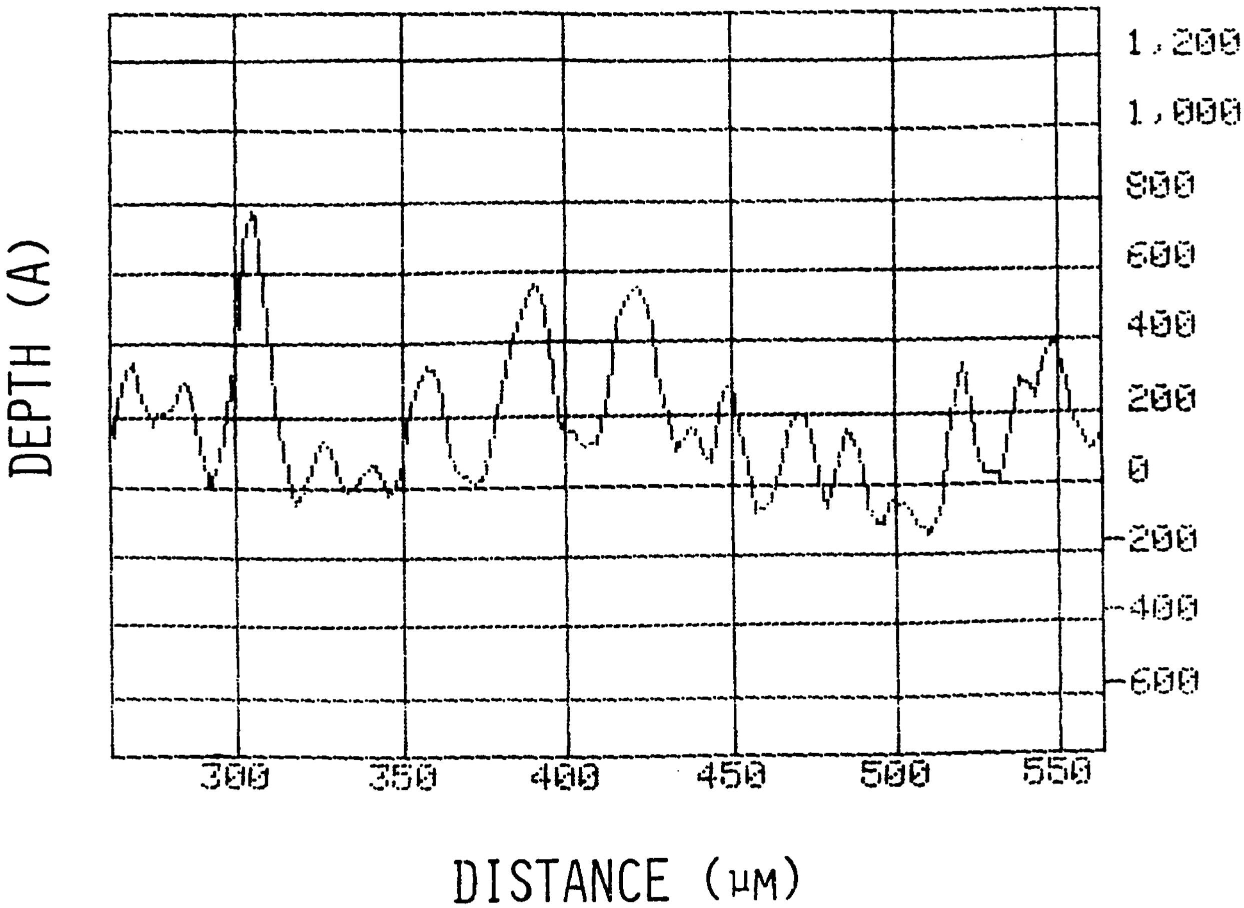
1,200
1,000
800
600
400
200
0
-200
-400
-600
DEPTH (Å)
300
350
400
450
500
550
DISTANCE (μM)

Figure 11.

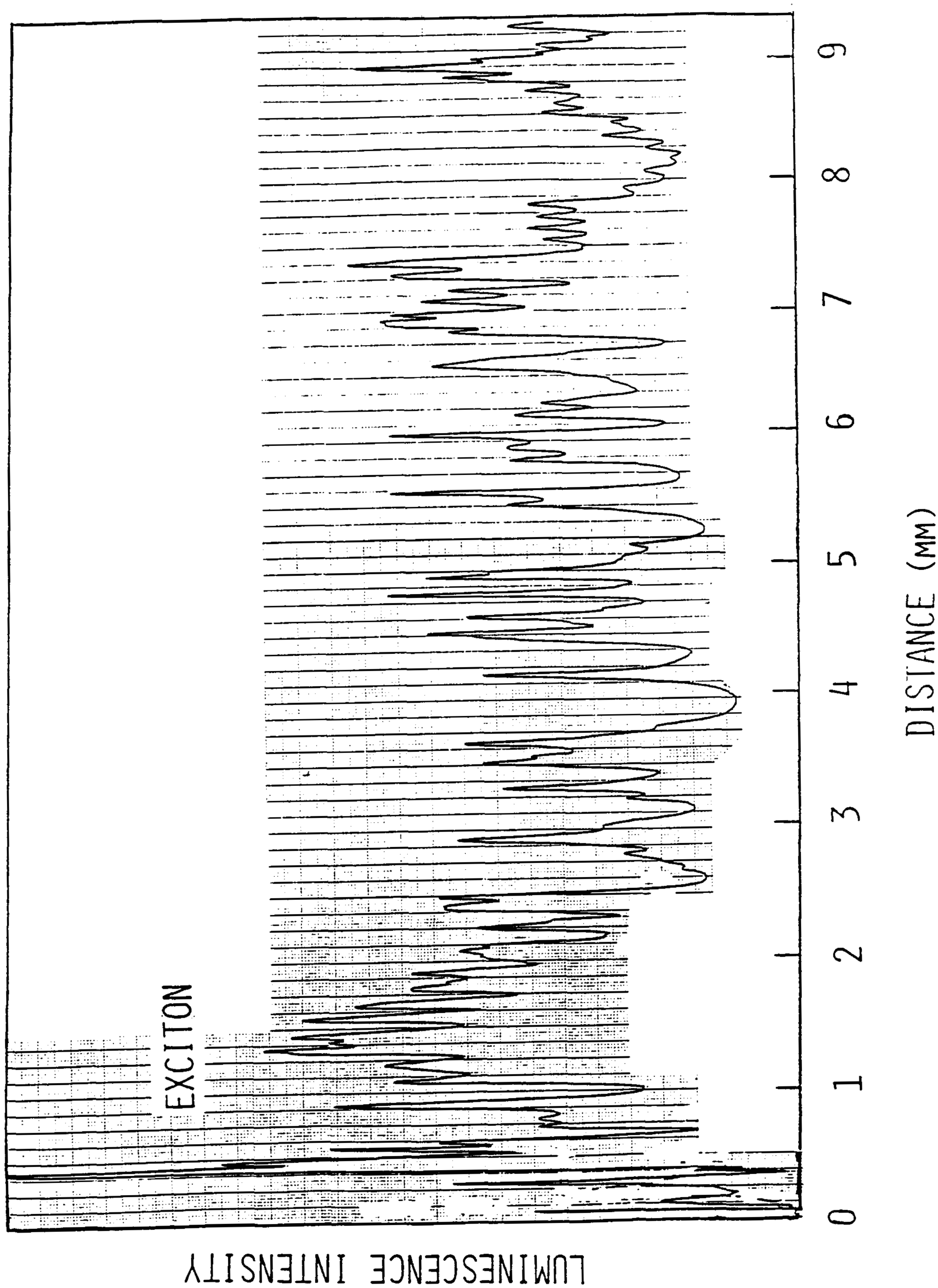

Figure 12.

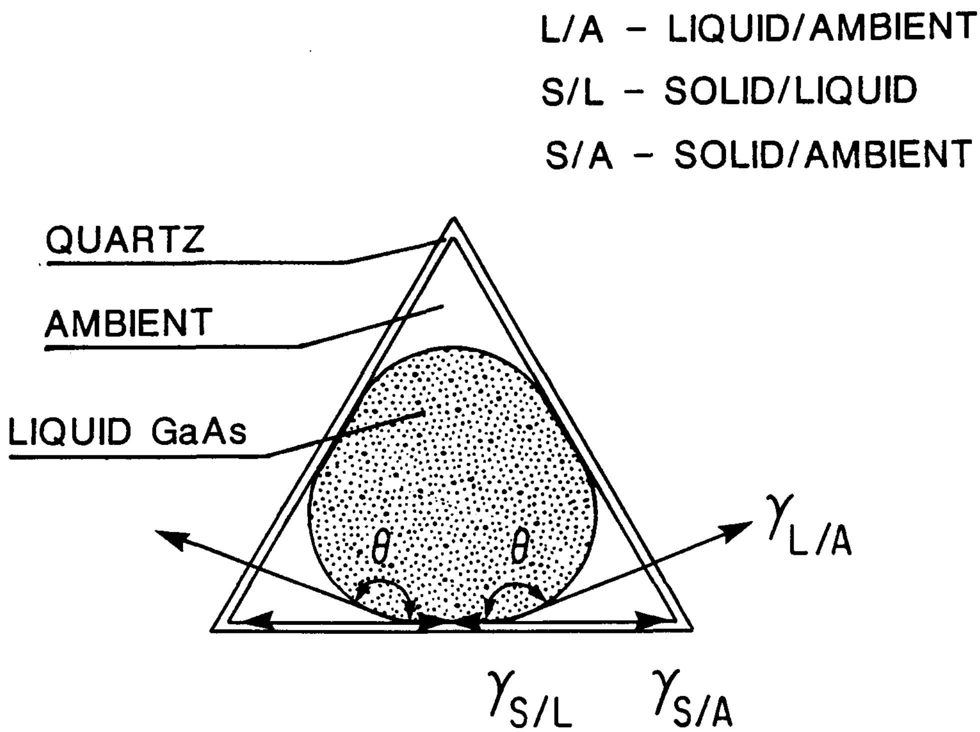
L/A - LIQUID/AMBIENT
S/L - SOLID/LIQUID
S/A - SOLID/AMBIENT
QUARTZ
AMBIENT
LIQUID GaAs
θ
θ
$\gamma_{L/A}$
$\gamma_{S/L}$
$\gamma_{S/A}$

Figure 13.

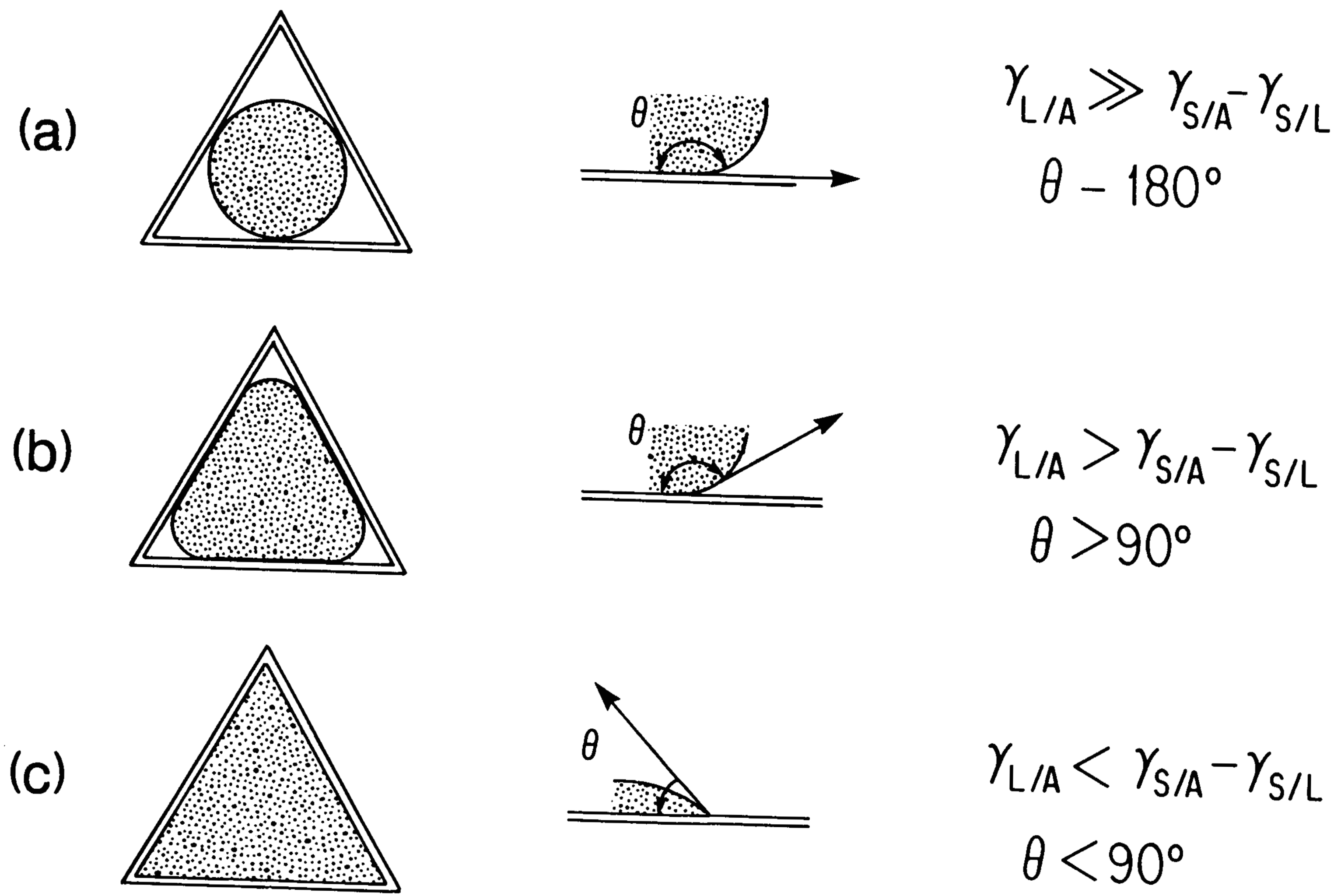
(a)
θ
$\gamma_{L/A} \gg \gamma_{S/A} - \gamma_{S/L}$
$\theta - 180°$
(b)
θ
$\gamma_{L/A} > \gamma_{S/A} - \gamma_{S/L}$
$\theta > 90°$
(c)
θ
$\gamma_{L/A} < \gamma_{S/A} - \gamma_{S/L}$
$\theta < 90°$

Figure 14.

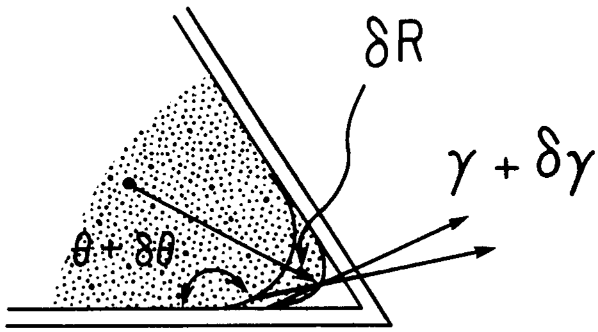

A small change in γ will change the contact angle, θ and the cross section of the liquid column

$$\frac{\delta R}{R} \simeq - \frac{\delta\gamma}{\gamma} \cos\theta$$

Figure 15.

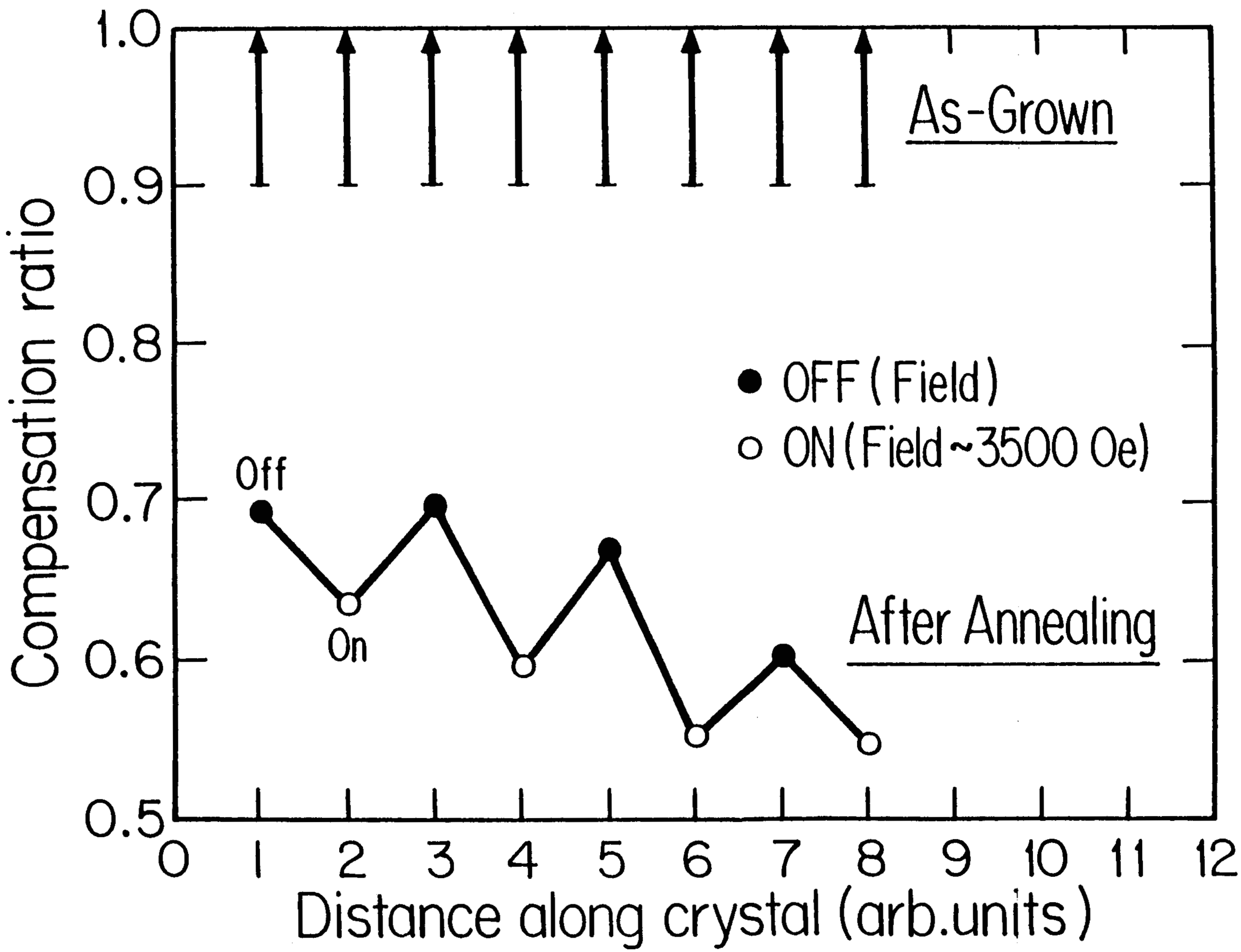
1.0
0.9
0.8
0.7
0.6
0.5
Compensation ratio
As-Grown
OFF (Field)
ON (Field ~3500 Oe)
Off
On
After Annealing
0 1 2 3 4 5 6 7 8 9 10 11 12
Distance along crystal (arb.units)

Figure 16.

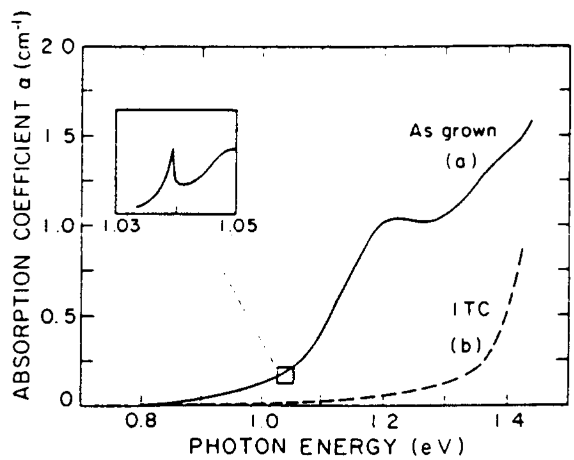
ABSORPTION COEFFICIENT α (cm⁻¹)
2.0
1.5
1.0
0.5
0
1.03
1.05
As grown
(a)
ITC
(b)
0.8
1.0
1.2
1.4
PHOTON ENERGY (eV)

Figure 17.